

Identification of a family of calcium sensors as protein ligands of inositol trisphosphate receptor Ca^{2+} release channels

Jun Yang*, Sean McBride*, Don-On Daniel Mak*, Noga Vardi†, Krzysztof Palczewski^{‡§¶}, Françoise Haeseleer[‡], and J. Kevin Foskett^{*||}

Departments of *Physiology and †Neuroscience, University of Pennsylvania, Philadelphia, PA 19104-6085; and Departments of ‡Ophthalmology, §Pharmacology, and ¶Chemistry, University of Washington, Seattle, WA 98195

Edited by David H. MacLennan, University of Toronto, Toronto, Canada, and approved March 26, 2002 (received for review January 4, 2002)

The inositol trisphosphate (InsP_3) receptor (InsP_3R) is a ubiquitously expressed intracellular Ca^{2+} channel that mediates complex cytoplasmic Ca^{2+} signals, regulating diverse cellular processes, including synaptic plasticity. Activation of the InsP_3R channel is normally thought to require binding of InsP_3 derived from receptor-mediated activation of phosphatidylinositol lipid hydrolysis. Here we identify a family of neuronal Ca^{2+} -binding proteins as high-affinity protein agonists of the InsP_3R , which bind to the channel and activate gating in the absence of InsP_3 . CaBP/caldendrin, a subfamily of the EF-hand-containing neuronal calcium sensor family of calmodulin-related proteins, bind specifically to the InsP_3 -binding region of all three InsP_3R channel isoforms with high affinity ($K_a \approx 25$ nM) in a Ca^{2+} -dependent manner ($K_a \approx 1$ μM). Binding activates single-channel gating as efficaciously as InsP_3 , dependent on functional EF-hands in CaBP. In contrast, calmodulin neither bound with high affinity nor activated channel gating. CaBP1 and the type 1 InsP_3R associate in rat whole brain and cerebellum lysates, and colocalize extensively in subcellular regions in cerebellar Purkinje neurons. Thus, InsP_3R -mediated Ca^{2+} signaling in cells is possible even in the absence of InsP_3 generation, a process that may be particularly important in responding to and shaping changes in intracellular Ca^{2+} concentration by InsP_3 -independent pathways and for localizing InsP_3 -mediated Ca^{2+} signals to individual synapses.

The inositol trisphosphate signaling pathway is present in nearly all cells. Activation of phospholipase C by G-protein-coupled receptors and receptor tyrosine kinases results in the hydrolysis of the membrane lipid phosphatidylinositol 4,5-bisphosphate to two products, diacylglycerol and the water-soluble inositol 1,4,5-trisphosphate (InsP_3) (1). InsP_3 diffuses in the cytoplasm and binds to a receptor, the InsP_3R , an integral membrane protein in the endoplasmic reticulum (ER), activating it as a Ca^{2+} channel to liberate stored Ca^{2+} from the ER lumen into the cytoplasm. This rapid release of Ca^{2+} modulates the cytoplasmic free Ca^{2+} concentration ($[\text{Ca}^{2+}]_i$), providing a ubiquitous intracellular signal with highly complex features that endow it with high temporal and spatial specificity (1, 2). The InsP_3 -mediated $[\text{Ca}^{2+}]_i$ -signaling system regulates a diversity of cellular processes, including secretion, contraction, gene transcription, intercellular communication, membrane transport, and synaptic plasticity (1, 3).

The ability of the InsP_3 signaling pathway to be at once ubiquitously expressed but nevertheless provide highly specific spatiotemporal $[\text{Ca}^{2+}]_i$ signals has been attributed to the diversity of InsP_3R isoform expression (4, 5), subcellular distributions of the InsP_3R channels (6–10), and complex regulation of the channel by both InsP_3 and $[\text{Ca}^{2+}]_i$ (1, 11, 12). Gating of the InsP_3 -liganded InsP_3R channel is modulated with a biphasic dependence on $[\text{Ca}^{2+}]_i$ (13–15). Importantly, Ca^{2+} binding to specific sites associated with the channel is necessary for InsP_3 to activate the channel. The requirement for Ca^{2+} binding enables the InsP_3R to participate in Ca^{2+} -induced Ca^{2+} release

(CICR), believed to be the fundamental feature that determines the spatial extent and magnitude of InsP_3 -induced $[\text{Ca}^{2+}]_i$ signals (2, 16). Furthermore, the requirement for both InsP_3 and Ca^{2+} binding enables the channel to function as a coincidence detector, which is believed to be important in determining the fidelity of signaling and in physiological processes, including synaptic plasticity (17). Here, we show that a family of Ca^{2+} sensor proteins (CaBPs) can relieve the requirement for InsP_3 in InsP_3R channel activation by acting as direct ligands of the channel. CaBPs bind to the InsP_3 -binding domain of the channel with high affinity in a Ca^{2+} -sensitive manner and activate channel gating in the absence of InsP_3 .

Materials and Methods

Yeast Two-Hybrid. The cDNA encoding the NH₂-terminal 600 aa of the rat InsP_3R -3 was cloned into pLexA and used as a bait to screen a human brain cDNA library (Invitrogen). Identification of positive colonies from $\approx 6 \times 10^6$ primary transformants, recovery of library plasmids, and identification of prey sequences were performed according to the manufacturer's instructions (CLONTECH) and as described (18). Positive plasmids were confirmed by retransformation. Nonspecific interactions were detected by cotransformation with library plasmids and the pLexA vector.

Cell Culture, Molecular Biology, and Biochemistry. COS-7 (*Cercopithecus aethiops* kidney) cells, grown in DMEM/high-glucose medium containing 10% FBS (GIBCO/BLR), were transfected with Lipofectamine (GIBCO/BLR) according to manufacturer's instructions. After 60 h, the cells were washed twice with $1 \times$ PBS and harvested in 1 ml of lysis buffer (10 mM Hepes, 250 mM NaCl, pH 7.1, 1% Triton X-100, and protease inhibitors). Coimmunoprecipitation and Western blotting were performed according to standard protocols. Unless specified, the Ca^{2+} concentration was estimated as ≈ 80 μM in lysates used in coimmunoprecipitation experiments. pGST-CaBP1 was constructed by cloning the cDNA corresponding to residues 19 to the COOH terminus (numbering based on s-CaBP1) from a positive clone in pYESTrp into the pGEX-6P-1 vector (Amersham Pharmacia). Glutathione S-transferase (GST)-CaBP1 was expressed in BL-21 (Stratagene) and purified on glutathione-Sepharose 4B (Amersham Pharmacia). Lysates, prepared from *Xenopus* oocytes as described (14, 19) and supplemented with an additional 100 mM NaCl and 500 μM free Ca^{2+} (4.5 mM EGTA,

This paper was submitted directly (Track II) to the PNAS office.

Abbreviations: InsP_3 , inositol trisphosphate; InsP_3R , inositol trisphosphate receptor; $[\text{Ca}^{2+}]_i$, cytoplasmic free Ca^{2+} concentration; Po, open probability; GFP, green fluorescent protein; ER, endoplasmic reticulum; GST, glutathione S-transferase; NCBP, neuronal Ca^{2+} -binding protein.

See commentary on page 7320.

¶To whom reprint requests should be addressed. E-mail: foskett@mail.med.upenn.edu.

5 mM Ca^{2+}), were incubated with the GST-CaBP1 for 1 h at 4°C. The beads were centrifuged to remove the supernatant, washed three times with lysis buffer, and prepared for Western blot analysis. $\Delta 1-600$ -InsP₃R-3 was constructed in a modified pSP64 vector (pSP-InsP₃R-3- $\Delta 1-600$) by PCR-amplification from pSP-InsP₃R-3 (19). Production of mRNA and its injection into oocytes were performed as described (14, 19). CaBP1 (residues 19 to the COOH terminus) was removed from GST-CaBP1 by digestion with PreScission protease (Amersham Pharmacia), and after elimination of the protease by using GSH-Sepharose 4B, it was dialyzed with Path buffer (10 mM Hepes/140 mM KCl, pH 7.2) and concentrated by using a 5 kDa concentrator (Millipore). Purified s-CaBP1 protein was prepared as described (20).

Electrophysiology. Patch-clamp experiments were performed by using isolated *Xenopus* oocyte nuclei as previously described (7, 13, 21, 22). Single-channel currents were amplified with anti-aliasing filtering at 1 kHz and digitized at 5 kHz. Pipette solutions contained 140 mM KCl and 10 mM Hepes with pH adjusted to 7.1 by using KOH. By using K^+ as the current carrier and appropriate quantities of the high-affinity Ca^{2+} chelator BAPTA (1,2-bis(*o*-aminophenoxy)ethane-*N,N,N',N'*-tetraacetic acid) (100–1000 μM), or the low-affinity Ca^{2+} chelator 5,5'-dibromo-BAPTA (100–400 μM), or ATP (0.5 mM) alone to buffer Ca^{2+} in the experimental solutions, free Ca^{2+} concentrations were tightly controlled. Bath solutions had 140 mM KCl, 10 mM Hepes, 380 μM CaCl_2 , 500 μM BAPTA ($[\text{Ca}^{2+}] = 500$ nM), and pH 7.1. Only single-channel records of sufficient duration were used in analysis of open probability (P_o).

Immunofluorescence Microscopy. Because antibodies to both InsP₃R and CaBP were raised in rabbits, rat brain sections were incubated sequentially as follows: CaBP1 antibody, excess goat anti-rabbit Fab' fragments conjugated to FITC (to cover all rabbit epitopes), InsP₃R-1 antiserum, and goat anti-rabbit IgG conjugated to rhodamine. Control experiments were similar except that antiserum against InsP₃R-1 was omitted. CaBP1-staining was specific because it was blocked by preabsorbing the antibody with CaBP1 peptide. Binding of the rhodamine-conjugated anti-rabbit antibody to the anti-CaBP1 antibody was insignificant, as demonstrated by the absence of labeling of stellate cells (see Results) with the rhodamine dye. Images were obtained with a Confocal Microscope (Leica).

Results

Identification of CaBPs as InsP₃R-Interacting Proteins. To explore the possibility that InsP₃ and Ca^{2+} -coincidence detection by the InsP₃R channel could be regulated in cells through protein interactions with the channel, we used the yeast two-hybrid system to identify proteins that interact with the NH₂-terminal 600 aa of the rat type 3 InsP₃R (r-InsP₃R-3). This region is present on the cytoplasmic portion of the channel and contains the InsP₃-binding domain, believed to lie within a region extending approximately from residue 225 to residue 580 (23–25). We screened a human brain cDNA library and identified all 14 positive clones as COOH-terminal fragments of a previously described gene family termed CaBP (20). CaBPs, originally cloned from retinal cDNA libraries (20), belong to the neuronal Ca^{2+} -binding protein (NCBP) subset of EF-hand-containing proteins. NCBP family members include recoverin, hippocalcin, neuronal calcium sensor-1 (frequenin), visinin, VILIPs, GCAPs, and KChips (calsenilin) (20, 26). NCBPs are similar to calmodulin family members in having four EF-hand motifs, but they are distinguished in that one or two of the motifs may be nonfunctional in Ca^{2+} binding, and they frequently are myristoylated at the NH₂ terminus (20, 26). The CaBP subfamily is distinguished by its unique combination of functional EF-hand motifs, with the

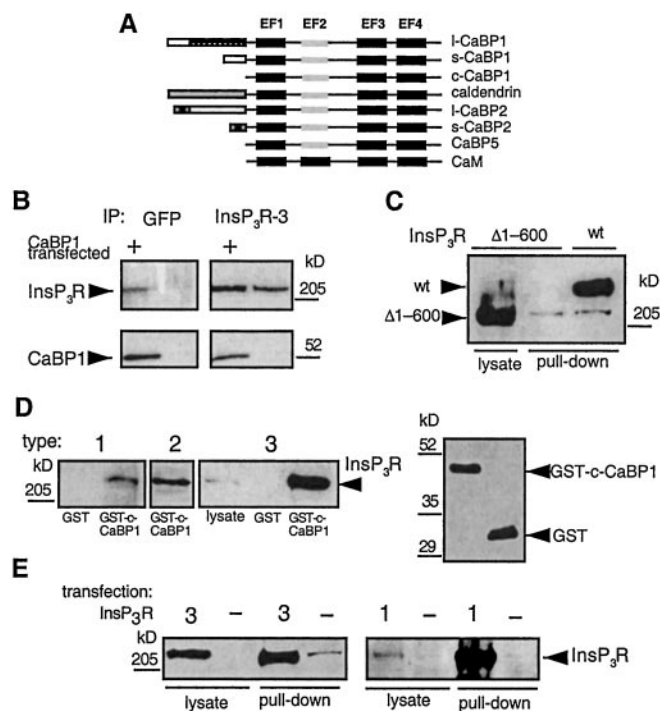


Fig. 1. Interaction of the InsP₃R with CaBP1. (A) Domain structures of CaBPs and calmodulin. (B) Coimmunoprecipitation of CaBP1 and InsP₃R-3 from control COS-7 cells (lanes 2 and 4) and COS-7 cells transiently transfected with s-CaBP1-GFP (lanes 1 and 3). Immunoprecipitates were probed with an InsP₃R type 3-specific antibody (Transduction Laboratories, Lexington, KY), (Upper) or anti-CaBP1 antibody (Lower). COS-7 cells do not express endogenous CaBP1 (lane 4). The InsP₃R-3 antibody does not interact with CaBP1 or GFP (not shown). (C) *In vitro* binding of InsP₃R-3 to CaBP1 requires the NH₂-terminal 600 residues of the InsP₃R. Lysates from *Xenopus* oocytes expressing full-length r-InsP₃R-3 (lane 3, lysate from 50 oocytes) or type 3 InsP₃R lacking the first 600 residues ($\Delta 1-600$ -InsP₃R-3) (lane 2, lysate from 50 oocytes) were incubated with GST-CaBP1, and bound InsP₃R was detected with a COOH-terminal InsP₃R-3 antibody (49). Expression of $\Delta 1-600$ -InsP₃R-3 was verified by immunoprecipitation and Western blotting (lane 1, lysate from 14 oocytes). (D) All three mammalian InsP₃R isoforms interact with CaBP1 *in vitro*. COS-7 cell lysates were incubated with GST-c-CaBP1, and bound InsP₃R was detected with isoform-specific antibodies. Type 1 was pulled down with GST only (in 5 mg of lysate, lane 1) or with GST-c-CaBP1 (from 5 mg of lysate, lane 2), type 2 in GST-c-CaBP1 pull-down from 1.25 mg of lysate (lane 3), and type 3 present in 50 μg of lysate (lane 4), in pull-down with GST only (from 1.25 mg of lysate) and in pull-down with GST-c-CaBP1 (from 1.25 mg of lysate). Equivalent GST-fusion protein concentrations were present in *in vitro* binding reactions as shown in Right a Western blot with anti-GST antibody (Amersham Pharmacia). Intensities are within the linear range. Inspection of intensities and normalization of lysates used indicate stoichiometric interaction of InsP₃R and CaBP1. (E) Homotetrameric rat types 1 and 3 InsP₃R isoforms interact with CaBP1. Lysates from control COS-7 cells (-) or COS-7 cells transfected with types 3 (3, Left) or 1 (1, Right) InsP₃R was incubated with GST-CaBP1, and bound InsP₃R was detected with isoform-specific antibodies. Type 3 (Left): 5 μg or 250 μg of cell lysate used in first and second pairs of lanes, respectively. Type 1 (Right): 25 μg or 250 μg of cell lysate used in third and fourth pairs of lanes, respectively. Because of high level overexpression of the InsP₃R, pull-down intensity is not proportional to the amount of InsP₃R input in this experiment.

second EF-hand disabled, and by the presence of an extra turn in the central α -helix. Five members have been identified: CaBP1–5 (20) (Fig. 1A). Alternative splicing of the NH₂-terminal regions also generates long and short forms of CaBP1 and CaBP2 (20). Another identified protein from this family termed caldendrin may represent a third splice variant of CaBP1 (20, 27). A protein containing the distal two EF-hands has been termed calbrain (28) but it is probably a partial clone of CaBP1

(20). Our screen identified caldendrin and CaBP1, which share identical COOH termini containing the EF-hand motifs. The longest clone identified in our two hybrid screen encompassed the COOH-terminal 256 aa containing all four EF-hands, whereas the shortest clone represented the COOH-terminal 103 aa containing three EF-hands, suggesting that CaBP1 and caldendrin interacted with the *InsP₃*-binding region of the r-*InsP₃*-R-3 through their COOH-terminal EF-hand-containing region.

To confirm in mammalian cells the protein interactions detected in yeast, a green fluorescent protein (GFP)-tagged short splice variant of human CaBP1 (s-CaBP1-GFP) (20) (Fig. 1B) was expressed in COS-7 cells, which endogenously express the *InsP₃*-R-3 (29). Immunoprecipitation of the *InsP₃*-R-3 with an isoform-specific monoclonal antibody efficiently coprecipitated CaBP1, detected by using a CaBP1 polyclonal antibody (Fig. 1B, lane 3). In the reciprocal experiment, immunoprecipitation of CaBP1 with an anti-GFP antibody (Chemicon) coprecipitated *InsP₃*-R-3 (Fig. 1B, lane 1). These results confirm and extend the observations in yeast by demonstrating that the full-length proteins can interact.

To determine whether the NH₂-terminal 600 residues used in the two-hybrid screen represented the only region of the *InsP₃*-R involved in the binding to CaBP1, *in vitro* “pull-down” assays were used. The conserved COOH terminus of CaBP1/caldendrin (c-CaBP1) was fused to GST to generate a fusion protein (GST-c-CaBP1) that was coupled to glutathione-Sepharose beads. Full-length r-*InsP₃*-R-3 or a mutant type 3 *InsP₃*-R lacking the first 600 residues (Δ 1–600-*InsP₃*-R-3) was expressed in *Xenopus* oocytes (Fig. 1C, lanes 3 and 1, respectively), which lack an endogenous type 3 receptor (19), and cellular lysates were passed over the GST-c-CaBP1 column. The full-length *InsP₃*-R-3 was efficiently pulled down by GST-c-CaBP1 (Fig. 1C, lane 3), whereas the Δ 1–600-*InsP₃*-R-3 was not detected in the pull-down (Fig. 1C, lane 2). Therefore, amino acids contained within the NH₂-terminal 600 residues of the *InsP₃*-R-3 are both necessary and sufficient for the interaction with CaBP1. These results also demonstrate that the conserved COOH-terminal region of CaBP1/caldendrin containing the four EF-hands mediates the binding, as inferred from the two-hybrid results.

The NH₂-terminal ligand-binding region used in the two-hybrid screen is conserved among the three different *InsP₃*-R isoforms (30), suggesting that in addition to the type 3 receptor, CaBP1/caldendrin might bind to the corresponding regions in the other two isoforms as well. To determine whether CaBP1 also binds to other *InsP₃*-R isoforms, GST-CaBP1 was used in pull-down experiments by using lysates from COS-7 cells, which express predominantly the types 2 and 3 *InsP₃*-R isoforms as well as low levels of *InsP₃*-R-1 (29). All three channel isoforms bound to CaBP1 (Fig. 1D). Given its low level of expression (29), the efficient pull-down of the endogenous type 1 isoform from COS-7 cell lysates (Fig. 1D, lane 2) suggests that the CaBP1–*InsP₃*-R interaction is a high-affinity one. However, because *InsP₃*-R isoforms may exist in hetero-oligomeric complexes, it was possible that the efficient pull-down of the type 1 isoform was indirect, due to its association with the endogenous type 3 isoform bound to CaBP1. Because transiently expressed recombinant types 1 and 3 *InsP₃*-Rs do not associate in hetero-oligomeric complexes with the endogenous *InsP₃*-Rs in COS-7 cells (29), we transfected COS-7 cells with r-*InsP₃*-R-1 and determined whether the expressed protein bound to CaBP1. As a control, r-*InsP₃*-R-3 was transiently expressed in parallel experiments. Both recombinant-channel isoforms efficiently bound to CaBP1 (Fig. 1E), demonstrating that CaBP1 can interact with homotetrameric types 1 and 3 *InsP₃*-R channels. Similar experiments were not performed with the type 2 isoform, but its high sequence homology with the other two isoforms suggests that it too likely binds directly to CaBP1/caldendrin.

The presence of EF-hand motifs suggests that CaBPs bind Ca²⁺. Ca²⁺-binding to NCBPs induces structural alterations that affect their binding to target proteins (26, 31). To investigate the functional significance of Ca²⁺ binding to CaBP1 on the interaction with the *InsP₃*-R, we treated s-CaBP1-GFP-expressing COS-7 cells with the Ca²⁺ ionophore ionomycin (2 μ M) for 2 min to raise [Ca²⁺]_i. Treatment with ionomycin enhanced the amount of s-CaBP1-GFP detected in *InsP₃*-R-3 immunoprecipitates (Fig. 2A), suggesting that Ca²⁺ enhances the interaction between the two proteins. The divalent cation dependencies of binding were investigated in more detail by fixing the concentrations of free Ca²⁺ and Mg²⁺ in COS-7 cell lysates, by using EGTA or EDTA buffers. In the absence of Ca²⁺, raising Mg²⁺ had little effect on binding (Fig. 2B, lane 1 vs. 2). In contrast, raising [Ca²⁺] to 500 μ M enhanced the binding of CaBP1 to the *InsP₃*-R (Fig. 2B, lane 3) by over 20-fold compared with that observed in the absence of Ca²⁺, although binding was still observed in the absence (\approx 2–5 nM) of Ca²⁺ (Fig. 2B, lane 2). To explore the requirement of Ca²⁺-binding to CaBP1 for optimal interaction of CaBP1 with the *InsP₃*-R, we mutated to alanine 6 conserved residues involved in Ca²⁺-coordination in functional EF-hands 1 (D96A, D98A), 3 (D173A, N175A), and 4 (D210A, N212A) [numbering based on the l-CaBP1 sequence (20)]. This CaBP1 triple-EF-hand mutant failed to bind to *InsP₃*-R-3, even in the presence of 500 μ M Ca²⁺ (Fig. 2C). Thus, Ca²⁺ binding to the functional EF-hands of CaBP1 appears to be required for optimal interaction with the *InsP₃*-R, although it is possible that Ca²⁺ binding to the *InsP₃*-R might affect the interaction of the two proteins. Wild-type CaBP1 binding to the *InsP₃*-R was strongly enhanced when [Ca²⁺] was raised from 100 nM to \approx 5 μ M (Fig. 2D), with an apparent Ca²⁺-affinity of \approx 1 μ M (Fig. 2E). Ca²⁺-induced CaBP1 binding to the *InsP₃*-R therefore occurs over a physiologically relevant range of [Ca²⁺]_i, suggesting that *in vivo* changes in [Ca²⁺]_i may dynamically regulate the interaction between the two proteins.

CaBPs Are Protein Ligands of the *InsP₃*-R Channel. We explored the functional consequences of the interaction of CaBP1 with the *InsP₃*-R channel, by patch clamp recording of single-channel currents of endogenous *Xenopus* type 1 *InsP₃*-R channels in their native membrane environment in the outer membrane of isolated oocyte nuclei (7, 21). Robust channel activity of the *InsP₃*-R (Fig. 3A) is observed only when the solutions in the patch electrodes contain *InsP₃* and an appropriate [Ca²⁺] (7, 13), because the cytoplasmic side of the channel, which contains the *InsP₃*- and Ca²⁺-binding regions, faces into the pipette (cf. Fig. 3E). To observe effects of CaBP1 on channel gating, purified s-CaBP1 or its COOH-terminal binding region (c-CaBP1) (1 μ M) together with *InsP₃* (33 nM) was included in the pipette solution at an optimal [Ca²⁺] (13). However, robust channel activity was similarly observed in the presence or absence of CaBP1 (Fig. 3B and C). Because CaBP1 interacts with the channel in a region that contains the *InsP₃*-binding domain, we also examined the effects of CaBP1 in the absence of *InsP₃*. Surprisingly, channel gating with high (P_o) (\approx 0.8) was observed when 1 μ M s-CaBP1 was included in the pipette solution (Fig. 3D, in 15 of 17 patches). The identification of the activated channels as *InsP₃*-Rs was based on the distinct conductance and gating properties of the channel in the oocyte nuclear membrane. Activation of gating was caused by CaBP1, because patches obtained from the same regions of the nucleus using pipettes lacking CaBP1 did not display channel activities (Fig. 3E, in 33 of 36 patches). The CaBP1 triple-EF-hand mutant protein (1 μ M) failed to activate the channel (Fig. 3F, in 10 of 11 patches). In contrast, channel gating was activated in the same membrane areas when the pipette solution contained CaBP1 in lieu of the CaBP1 triple-EF-hand mutant protein (Fig. 3G, in 12 of 12 patches), which demonstrated that the failure to observe

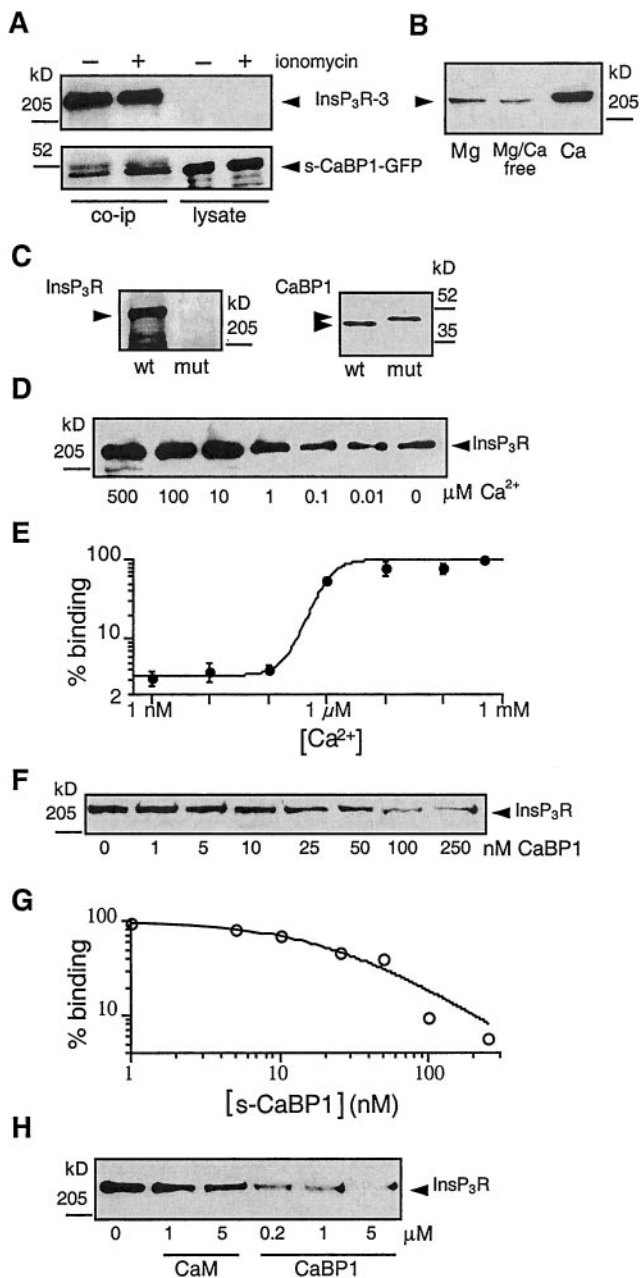


Fig. 2. Ca^{2+} dependence of CaBP1- InsP_3R interaction. (A) Elevation of $[\text{Ca}^{2+}]_i$ enhances the interaction of the InsP_3R with CaBP1. Coimmunoprecipitation, using type 3 InsP_3R antibody, of CaBP1 with InsP_3R -3 from lysates of CaBP1-GFP-transfected COS-7 cells (Left) exposed (+) or not (-) for 2 min to the Ca^{2+} -ionophore ionomycin ($2 \mu\text{M}$). Immunoprecipitates (Left) or cell lysates (Right; $5 \mu\text{g}$ each) were probed for InsP_3R -3 (Upper) or CaBP1 (Lower). Ionomycin enhanced the amount of CaBP1 detected in immunoprecipitates, which contained equal amounts of InsP_3R (lanes 1 and 2, Top) and s-CaBP1-GFP (lanes 3 and 4, Bottom). (B) *In vitro* binding of InsP_3R -3 to CaBP1 is specifically enhanced by Ca^{2+} . COS-7 cell lysates, with free $[\text{Mg}^{2+}]$ and $[\text{Ca}^{2+}]$ fixed to $500 \mu\text{M}$ $\text{Mg}^{2+}/0 \text{Ca}^{2+}$ (left lane), $0 \text{Mg}^{2+}/0 \text{Ca}^{2+}$ (center lane) or $0 \text{Mg}^{2+}/500 \mu\text{M}$ Ca^{2+} (right lane) were incubated with GST-c-CaBP1, and bound InsP_3R was detected with type-3-specific antibody. (C) Functional Ca^{2+} -binding EF-hands are required for CaBP1 to interact with the InsP_3R . Endogenous InsP_3R -3 from COS-7 cell lysate was pulled down with GST-CaBP1 (wt) but not with GST-CaBP1 triple-EF-hand mutant (mut). Equivalent GST-fusion protein concentrations were present in *in vitro* binding reactions (Right, Coomassie stain). (D) $[\text{Ca}^{2+}]$ -dependence of *in vitro* interaction of CaBP1 and InsP_3R . Endogenous InsP_3R -3 in COS-7 cell lysate (1.25 mg) with $[\text{Ca}^{2+}]$ fixed as indicated was pulled down with GST-c-CaBP1 and probed with InsP_3R -3 antibody. (E) $[\text{Ca}^{2+}]_i$ -dependence of InsP_3R -3 interaction with CaBP1 by quantitative densitometry of gels similar to that shown in D ($n = 3$) with data normalized to binding observed in $500 \mu\text{M}$

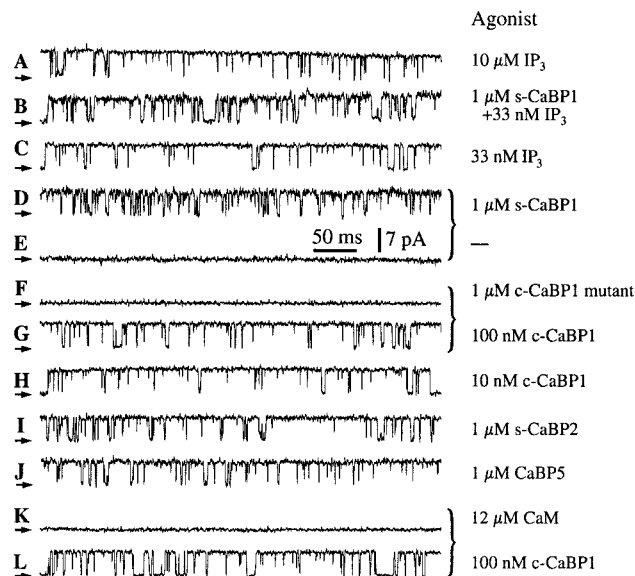


Fig. 3. Typical patch-clamp current records from outer membrane patches obtained from isolated *Xenopus* oocyte nuclei. Applied potential = 20 mV . The arrows indicate the closed-channel current level. The pipette solutions contained: $10 \mu\text{M}$ InsP_3 (A), 33 nM InsP_3 and $1 \mu\text{M}$ s-CaBP1 (B), 33 nM InsP_3 (C), $1 \mu\text{M}$ s-CaBP1 (D), no agonist (E), $1 \mu\text{M}$ CaBP1 triple-EF-hand mutant (F), 100 nM c-CaBP1 (G), 10 nM c-CaBP1 (H), $1 \mu\text{M}$ s-CaBP2 (I), $1 \mu\text{M}$ CaBP5 (J), $12 \mu\text{M}$ calmodulin (K), or 100 nM c-CaBP1 (L). Current traces D and E, F and G, and K and L (those indicated with braces) were recorded with membrane patches obtained from the same region of the same oocyte nuclei. Free Ca^{2+} concentrations used in all pipette solutions were optimal for achieving maximum channel P_o ($1.5\text{--}21 \mu\text{M}$; ref. 13). n = number of patches used to determine P_o . $P_o = 0.78 \pm 0.03$, $n = 12$ (A); $P_o = 0.65 \pm 0.06$, $n = 4$ (B); $P_o = 0.77 \pm 0.08$, $n = 5$ (C); $P_o = 0.78 \pm 0.03$, $n = 10$ (D); $P_o = 0.71 \pm 0.03$, $n = 9$ (G, L); $P_o = 0.70 \pm 0.06$, $n = 6$ (H); $P_o = 0.87 \pm 0.02$, $n = 7$ (I); $P_o = 0.87 \pm 0.02$, $n = 5$ (J).

channels by using pipettes lacking either InsP_3 or CaBP1 or containing the EF-hand mutant CaBP1 was not due to the absence of InsP_3R channels in the membrane patches. Thus, Ca^{2+} -dependent binding of CaBP1 to the InsP_3R (Fig. 2) mediates the activation of channel gating. CaBP1-dependent activation of InsP_3R channels with reasonably high P_o (≈ 0.7) was observed even with CaBP1 concentrations reduced to 10 nM (Fig. 3H). These electrophysiological results indicate that CaBP1 is a high-affinity activator of the InsP_3R . Taken together, our functional and biochemical results demonstrate that CaBP1 is a high-affinity, specific protein ligand of the InsP_3R , the Ca^{2+} -dependent binding of which activates channel gating in the absence of InsP_3 with features (P_o , gating kinetics) remarkably similar to those activated by InsP_3 (7, 32).

We examined the specificity of the effects of CaBP1 by performing electrophysiological studies using other CaBP family members. Purified bovine s-CaBP2 and mouse CaBP5 ($1 \mu\text{M}$ each) (20), with COOH-terminal sequences that are $\approx 85\%$ similar to human CaBP1/calendrin, each stimulated InsP_3R channel gating with high P_o in optimal $[\text{Ca}^{2+}]_i$ (Fig. 3 I and J).

Ca^{2+} . (F) CaBP1-binding affinity for the InsP_3R -3. Endogenous InsP_3R -3 was pulled down with GST-CaBP1 from COS-7 cell lysates (1.25 mg) containing defined concentrations of s-CaBP1. (G) Quantitative analysis of competition for CaBP1 binding to InsP_3R -3 by s-CaBP1 with data normalized to binding in the absence of added s-CaBP1. (H) Specificity of the interaction with the InsP_3R of CaBP1 vs. calmodulin (CaM). Endogenous COS-7 cell InsP_3R -3 was pulled down with GST-c-CaBP1 from lysates (1.25 mg) supplemented with various concentrations of CaM or s-CaBP1.

These results therefore identify the CaBP Ca^{2+} sensors as a family of protein ligands of the InsP_3R channel.

CaBP1/caldendrin as well as other NCBPs belong to a superfamily of EF-hand-containing proteins, of which calmodulin is the prototypical member. Calmodulin has been implicated in the regulation of the InsP_3R (33, 34) and some studies have suggested that calmodulin may affect InsP_3 binding to the channel, possibly by interacting with residues near or within the InsP_3 -binding region (34, 35). Calmodulin has $\approx 60\%$ sequence similarity over the CaBP1 region used in our binding and electrophysiology studies (20). To determine whether calmodulin could also bind to the CaBP1-interacting region of the InsP_3R , we performed *in vitro* binding competition experiments. Purified calmodulin or s-CaBP1 protein was added to COS-7 cell lysates, from which the InsP_3R -3 was pulled down by passage over a GST-c-CaBP1 column. s-CaBP1 competitively inhibited the binding of the InsP_3R -3 channel to GST-c-CaBP1 with an apparent affinity (half-maximal inhibition) of ≈ 25 nM (Fig. 2*F* and *G*). In contrast, calmodulin, even at high concentrations (5 μM), had relatively little effect on the binding (Fig. 2*H*), indicating that it does not interact well with the CaBP-binding site of the InsP_3R . Electrophysiological experiments were conducted with calmodulin (12 μM) included in the pipette solution. However, calmodulin never activated channel gating (Fig. 3*K*, in 17 of 17 patches) in membrane regions where c-CaBP1 did (Fig. 3*L*, in 13 of 14 patches), in accord with the protein-binding data. Thus, the interactions of CaBPs with the InsP_3R channel are highly specific ones that are not recapitulated by calmodulin.

CaBP1 and InsP_3R Interact and Colocalize in Brain. CaBP1 and caldendrin are expressed in specific cell types in the retina and throughout the brain, including cortex, cerebellum, and hippocampus (20, 27, 36, 37), whereas CaBP2, -3, and -5 may be retina-specific (20). Caldendrin expression in the brain appears to be restricted to neurons, where it has been localized to the somatodendritic compartment, with particular enrichment at dendritic postsynaptic densities (27, 36). The InsP_3R is widely distributed throughout the brain, with the type 1 isoform (InsP_3R -1) most highly expressed, and it is also localized in neuronal somatic and dendritic compartments (38–40). To verify the interaction of endogenous InsP_3R and CaBP1 in brain, we performed immunoprecipitation and colocalization experiments. CaBP1 was present in immunoprecipitates of InsP_3R -1 or InsP_3R -3 from whole rat brain (Fig. 4*A*). Immunoprecipitation of InsP_3R -1 from cerebellum, where it is expressed at very high levels in Purkinje cells (41, 42) coimmunoprecipitated CaBP1. Like InsP_3R -1, staining for CaBP1 in cerebellum was strong in Purkinje cell somas and in their dendrites in the molecular layer (Fig. 4*B*), with staining also present in small somas of stellate cells in the molecular layer, and in fine puncta in the granular cell layer. CaBP1 and InsP_3R -1 co-localized (within the ≈ 0.4 - μm optical resolution of the microscope) extensively in Purkinje cell somas and dendrites (Fig. 4*B* and *F*). Colocalization was nearly complete in dendrites, and in striated structures (Fig. 4*C* and *F*) that are most likely the smooth ER that runs parallel to the dendritic axis immediately adjacent to the plasma membrane (subsurface or hypolemmal cisternae) (41, 43). These results demonstrate that CaBP1 is membrane-localized, perhaps through its myristoylated N terminus, in close proximity to the InsP_3R in neurons.

Discussion

We have identified members of a subfamily of the neuronal Ca^{2+} -sensor protein family as high-affinity ligands of all of the mammalian isoforms of the InsP_3R Ca^{2+} release channel. Elevation of cytoplasmic $[\text{Ca}^{2+}]_i$ promotes binding of CaBPs to the region of the InsP_3R -channel that contains the InsP_3 -binding domain and activates channel gating in the absence of InsP_3 .

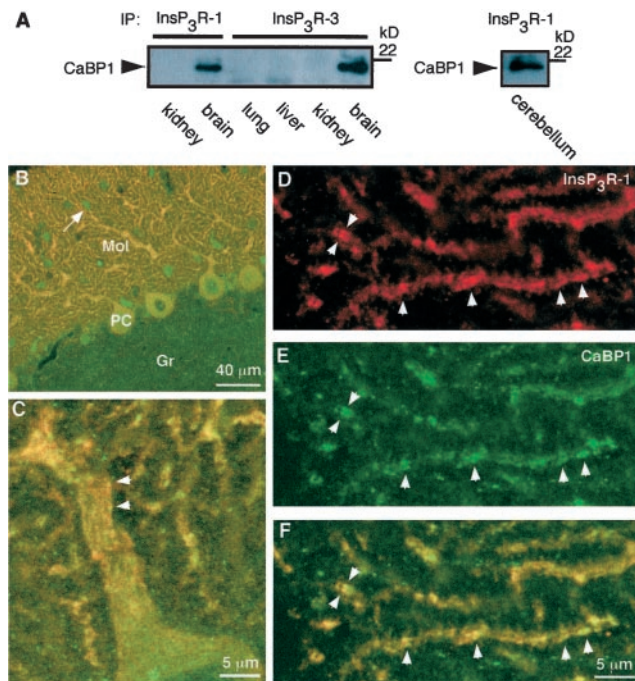


Fig. 4. Interaction of InsP_3R and CaBP1 in brain. (A) Coimmunoprecipitation of CaBP1 with InsP_3R -1 (Left and Right) or InsP_3R -3 (Left) from whole mouse brain (Left) and cerebellum (Right), but not from nonneural tissues (Left). Immunoprecipitates were probed with anti-CaBP1 antibody. The reciprocal experiment could not be performed because the CaBP antibody is directed against the same region to which the InsP_3R binds. (B–F) Confocal immunolocalization of InsP_3R -1 and CaBP1 in rat cerebellum sagittal sections. (B) Low magnification. CaBP1 (green) and InsP_3R -1 (red) are localized to Purkinje cell somas (PC) and their dendrites in the molecular layer (Mol) (colocalization indicated by yellow). CaBP1 (but not InsP_3R -1) is also localized to unidentified fine structures within the granular cell layer (Gr) and to stellate cells (arrow) in the molecular layer. (C–F) Higher magnification demonstrating subcellular colocalization on endoplasmic reticulum. (C) Striated colocalization (yellow) in Purkinje cell primary dendrite. (D–F) Dendritic tips of Purkinje cells. CaBP1 (E; green) and InsP_3R -1 (D; red) are colocalized (F; yellow) to linear subregions within thin dendrites (arrowheads).

The existence of protein ligands of the InsP_3R may suggest that InsP_3R -mediated Ca^{2+} signaling could be recruited under conditions in which the phosphoinositide signaling system remains unengaged. The InsP_3R , as well as the other major Ca^{2+} -release channel in cells, the ryanodine receptor, is activated by Ca^{2+} binding, enabling both to participate in Ca^{2+} -induced Ca^{2+} release (CICR), a process critical for their signaling functions. However, the InsP_3R has been distinguished from the ryanodine receptor by its requirement for ligand binding. Identification of CaBPs as ligands whose binding to the InsP_3R is promoted by Ca^{2+} may enable the channel to become activated by a rise of Ca^{2+} concentration without the necessity for InsP_3 and Ca^{2+} coincidence detection, thereby enabling it to be involved in regenerative Ca^{2+} release in a pure, albeit distinct, CICR process. Physiologically, such a mechanism may be important in amplifying Ca^{2+} signals generated by other mechanisms, including Ca^{2+} influx through the plasma membrane or release from other intracellular stores. For example, Ca^{2+} stores in excitable cells function as integrators and amplifiers of Ca^{2+} influx, roles that are particularly important in dendritic spines and in synaptic plasticity (3, 17). Induction of binding of CaBP to the InsP_3R by elevations of $[\text{Ca}^{2+}]_i$ due to Ca^{2+} influx through voltage-gated Ca^{2+} channels could provide Ca^{2+} -store-mediated amplification of the Ca^{2+} signal, thereby inducing synaptic

plasticity without the requirement for parallel activation of InsP_3 -generating receptor pathways.

Cerebellar Purkinje cells express very high levels of the $\text{InsP}_3\text{R-1}$, where it is involved in long-term depression (39, 44). Paradoxically, the channel is remarkably insensitive to InsP_3 in this cell type, so that Ca^{2+} release requires InsP_3 concentrations that are over two orders of magnitude higher than those required to gate the channel in electrophysiological studies (45). The molecular basis for the *in vivo* insensitivity of the channel to InsP_3 is unknown. The identification of CaBP proteins as ligands that interact with the InsP_3 -binding site of the channel may suggest a possible mechanism. The apparent close physical proximity of the InsP_3R and CaBP1 in Purkinje cells (Fig. 4) may enable CaBP to bind to the channel with high avidity even when cytoplasmic Ca^{2+} concentration is low under resting conditions. The channel in this state may be less sensitive to InsP_3 . Titration by CaBP of the effective affinity of InsP_3 could provide a

mechanism to ensure that InsP_3 -induced Ca^{2+} signals are generated and restricted to highly localized regions immediately adjacent to the sites of InsP_3 production, as observed at synaptic inputs in Purkinje cells (39).

Because InsP_3R -mediated Ca^{2+} signals are shaped by messenger diffusion, degradation, and removal, processes that will have distinct kinetics for InsP_3 compared with CaBPs, the identification of protein ligands for the InsP_3R provides insights into the dimensions and versatility of this ubiquitous signaling pathway.

We thank A. Tanimura and S. Joseph for antibodies, and M. Wallenstein for technical support. This work was supported by research grants from the National Institutes of Health (GM56328 and MH59937 to J.K.F.), American Heart Association (9906220U to D.-O.D.M.), Research to Prevent Blindness, Inc. (EY08061 to the Department of Ophthalmology, University of Washington), and the E.K. Bishop Foundation. K.P. is recipient of a Research to Prevent Blindness Senior Investigator Award.

1. Berridge, M. J. (1993) *Nature (London)* **361**, 315–325.
2. Berridge, M. J. (1997) *J. Exp. Biol.* **200**, 315–319.
3. Berridge, M. J., Bootman, M. D. & Lipp, P. (1998) *Nature (London)* **395**, 645–648.
4. Taylor, C. W., Genazzani, A. A. & Morris, S. A. (1999) *Cell Calcium* **26**, 237–251.
5. Patel, S., Joseph, S. K. & Thomas, A. P. (1999) *Cell Calcium* **25**, 247–264.
6. Hirose, K. & Iino, M. (1994) *Nature (London)* **372**, 791–794.
7. Mak, D.-O. D. & Foskett, J. K. (1997) *J. Gen. Physiol.* **109**, 571–587.
8. Barritt, G. J. (1999) *Biochem. J.* **337**, 153–169.
9. Lee, M. G., Xu, X., Zeng, W. Z., Diaz, J., Wojcikiewicz, R. J. H., Kuo, T. H., Wuytack, F., Racymaekers, L. & Muallem, S. (1997) *J. Biol. Chem.* **272**, 15765–15770.
10. Yamamoto-Hino, M., Miyawaki, A., Segawa, A., Adachi, E., Yamashina, S., Fujimoto, T., Sugiyama, T., Furuichi, T., Hasegawa, M. & Mikoshiba, K. (1998) *J. Cell Biol.* **141**, 135–142.
11. Thorn, P. (1996) *Cell Calcium* **20**, 203–214.
12. Bootman, M. D. & Berridge, M. J. (1995) *Cell* **83**, 675–678.
13. Mak, D.-O. D., McBride, S. & Foskett, J. K. (1998) *Proc. Natl. Acad. Sci. USA* **95**, 15821–15825.
14. Mak, D.-O. D., McBride, S. & Foskett, J. K. (2001) *J. Gen. Physiol.* **117**, 435–446.
15. Bezprozvanny, I., Watras, J. & Ehrlich, B. E. (1991) *Nature (London)* **351**, 751–754.
16. Marchant, J. S. & Parker, I. (2000) *J. Gen. Physiol.* **116**, 691–695.
17. Berridge, M. J. (1998) *Neuron* **21**, 13–26.
18. Hallows, K. R., Raghuram, V., Kemp, B. E., Witters, L. A. & Foskett, J. K. (2000) *J. Clin. Invest.* **105**, 1711–1721.
19. Mak, D.-O. D., McBride, S., Raghuram, V., Yue, Y., Joseph, S. K. & Foskett, J. K. (2000) *J. Gen. Physiol.* **115**, 241–255.
20. Haeseleer, F., Sokal, I., Verlinde, C. L. M. J., Erdjument-Bromage, H., Tempst, P., Pronin, A. N., Benovic, J. L., Fariss, R. N. & Palczewski, K. (2000) *J. Biol. Chem.* **275**, 1247–1260.
21. Mak, D.-O. D. & Foskett, J. K. (1994) *J. Biol. Chem.* **269**, 29375–29378.
22. Mak, D.-O. D. & Foskett, J. K. (1998) *Am. J. Physiol.* **275**, C179–C188.
23. Yoshikawa, F., Morita, M., Monkawa, T., Michikawa, T., Furuichi, T. & Mikoshiba, K. (1996) *J. Biol. Chem.* **271**, 18277–18284.
24. Mignery, G. A. & Sudhof, T. C. (1990) *EMBO J.* **9**, 3893–3898.
25. Miyawaki, A., Furuichi, T., Ryou, Y., Yoshikawa, S., Nakagawa, T., Saitoh, T. & Mikoshiba, K. (1991) *Proc. Natl. Acad. Sci. USA* **88**, 4911–4915.
26. Burgoyne, R. D. & Weiss, J. L. (2001) *Biochem. J.* **353**, 1–12.
27. Seidenbecher, C. I., Langnaese, K., Sanmarti-Vila, L., Boeckers, T. M., Smalla, K.-H., Sabel, B. A., Garner, C. C., Gundelfinger, E. D. & Kreutz, M. R. (1998) *J. Biol. Chem.* **273**, 21324–21331.
28. Yamaguchi, K., Yamaguchi, F., Miyamoto, O., Sugimoto, K., Konishi, R., Hatase, O. & Tokuda, M. (1999) *J. Biol. Chem.* **274**, 3610–3616.
29. Joseph, S. K., Bokkala, S., Boehning, D. & Zeigler, S. (2000) *J. Biol. Chem.* **275**, 16084–16090.
30. Mikoshiba, K. (1993) *Trends Pharmacol. Sci.* **14**, 86–89.
31. Sokal, I., Li, N., Verlinde, C. L. M. J., Haeseleer, F., Baehr, W. & Palczewski, K. (2000) *Biochim. Biophys. Acta* **1498**, 233–251.
32. Mak, D.-O. D., McBride, S. & Foskett, J. K. (2001) *J. Gen. Physiol.* **117**, 299–314.
33. Michikawa, T., Hirota, J., Kawano, S., Hiraoka, M., Yamada, M., Furuichi, T. & Mikoshiba, K. (1999) *Neuron* **23**, 799–808.
34. Adkins, C. E., Morris, S. A., De Smedt, H., Sienaert, I., Török, K. & Taylor, C. W. (2000) *Biochem. J.* **345**, 357–363.
35. Sipma, H., De Smet, P., Sienaert, I., Vanlingen, S., Missiaen, L., Parys, J. B. & De Smedt, H. (1999) *J. Biol. Chem.* **274**, 12157–12162.
36. Menger, N., Seidenbecher, C. I., Gundelfinger, E. D. & Kreutz, M. R. (1999) *Cell Tissue Res.* **298**, 21–32.
37. Haverkamp, S. & Wassle, H. (2000) *J. Comp. Neurol.* **424**, 1–23.
38. Sharp, A. H., Dawson, T. M., Ross, C. A., Fotuhi, M., Mourey, R. J. & Snyder, S. H. (1993) *Neuroscience* **53**, 927–942.
39. Finch, E. A. & Augustine, G. J. (1998) *Nature (London)* **396**, 753–756.
40. Furuichi, T. & Mikoshiba, K. (1995) *J. Neurochem.* **64**, 953–960.
41. Ross, C. A., Meldolesi, J., Milner, T. A., Satoh, T., Supattapone, S. & Snyder, S. H. (1989) *Nature (London)* **339**, 468–470.
42. Otsu, H., Yamamoto, A., Maeda, N., Mikoshiba, K. & Tashiro, Y. (1990) *Cell Struct. Funct.* **15**, 163–173.
43. Peters, A., Palay, L. S. & Webster, H. (1991) *The Fine Structure of the Nervous System. Neurons and Their Supporting Cells* (Oxford Univ. Press, Oxford).
44. Khodakhah, K. & Armstrong, C. M. (1997) *Proc. Natl. Acad. Sci. USA* **94**, 14009–14014.
45. Khodakhah, K. & Ogden, D. (1993) *Proc. Natl. Acad. Sci. USA* **90**, 4976–4980.